Proceedings of the Sixth International Conference on
Railway Technology: Research, Development and Maintenance
Edited by: J. Pombo
Civil-Comp Conferences, Volume 7, Paper 4.5
Civil-Comp Press, Edinburgh, United Kingdom, 2024
ISSN: 2753-3239, doi: 10.4203/ccc.7.4.5

A Model Predictive Controller for Hardware-in-the-Loop Pantograph Test

M. Tur[1], S. Gregori[1], P. Antunes[2], J. P. Santos[2], A. M. Pedrosa[1], J. Gil Romero[1] and J. Pombo[2,3,4]

[1]Institute of Mechanical Engineering and Biomechanics, Universitat Politecnica de Valencia, Spain
[2]Institute of Railway Research, School of Computing and Engineering, University of Huddersfield, UK
[3]IDMEC, Instituto Superior Técnico, Universidade de Lisboa, Portugal
[4]ISEL, Instituto Politecnico de Lisboa, Portugal

Abstract

Hardware-in-the-loop testing serves as a means of analysing the dynamic interaction between the pantograph and catenary in controlled laboratory settings. The process starts measuring the force from the pantograph and determines the next pantograph's virtual position using a real-time catenary model. The position is sent to an actuator, generating the desired pantograph movement to complete the loop. This work proposes a new catenary model and a Model Predictive Controller to address instability issues arising from communication delays and interaction stiffness. The method is validated experimentally through tests with a DSA-380 pantograph. The results demonstrate an acceptable accuracy of the test results in the frequency range of 0-20 Hz.

Keywords: pantograph, catenary, hardware-in-the-loop test, model predictive controller, real-time, test rig

1 Introduction

Hardware-in-the-Loop (HiL) is a technique employed to evaluate the performance of pantograph in the laboratory. This is important to guarantee the safety and reliability of the railway system. In this work, we propose a HiL method for testing the pantograph-catenary interaction, using a simplified real-time catenary model allowing the application of a Model Predictive Controller (MPC) to stabilise the control loop.

The literature explores diverse approaches for HiL testing, using different catenary models, actuation methods, and control technologies. Polimi test rig [1] includes an electrohydraulic actuator and an electric motor to simulate vertical and lateral catenary movement, respectively. The catenary model consists of tensioned wires connected by non-linear droppers, with a shift-forward strategy for emulating longer catenaries. TUW's approach, presented by Schirrer et al. [2], introduces a more complex catenary model with MPC, with correction of the position and force to stabilise the system.

Kobayashi et al. [3] at RTRI use a lumped-mass catenary model and a servohydraulic actuator. A substructure control algorithm is introduced to address delays, ensuring stability and more realistic testing.

UPV [4] defines a periodic finite element catenary model with non-linear droppers and a new delay compensation technique, leading to accurate results in the 0-25 Hz frequency range.

In general terms, the previous works use a periodic catenary model in HiL tests, and testing results are compared in the 0-20 Hz frequency range. In the present work, a complete catenary section is defined, including general geometry with different number of droppers per span, contact height variability, etc.

The next section briefly explains the catenary model proposed, the test rig components, and the controller used to stabilise the system. Section 3 presents the validation of the proposed methodology and some HiL test results of a DSA-380 pantograph. Conclusions and contributions are summarised in Section 4.

2 Methods

2.1 HiL Tests

Figure 1 shows the HiL test workflow, and Figure 2 shows the test rig components. A more detailed description of the test rig components can be found in [5]. A linear motor (2) is located in the central part of the main structure built with aluminium profiles. The motor reproduces the vertical displacement of the contact point of the catenary, and a second horizontal guide and motor (3) reproduces the lateral movement due to the wind and contact wire staggering. Two load cells (4) located at the ends of the linear motor slider, interact with the pantograph contact strips. The measured contact force is sent to the Speedgoat calculation PC (5) containing the virtual catenary model. The dynamic response of a time step of the virtual catenary is simulated in real time, resulting in the height of the contact wire at the next contact point. This height is the control signal sent to the linear motor, through the control system, which will modify its position and, therefore, the interaction force with the pantograph. This procedure is repeated at each time step, closing the loop.

Tests are managed by a real-time NI-cRIO that ensures a constant time step and synchronization of the system. The control real-time NI-cRIO has an integrated acquisition system that is responsible for obtaining both the force measured by the load cells and the position control of the linear motor (6). The pantograph (1) is a DSA-380 model actioned by a pneumatic circuit (7).

Due to communication, there are two one-step delays: the contact force received by the PC and the computed position reference sent to the motor driver. Because of these delays and the high stiffness of the contact pads, the system can become unstable. The stability and delay compensation were analysed in [8]. Here, we adopt an approach more aligned with [7], including an MPC controller.

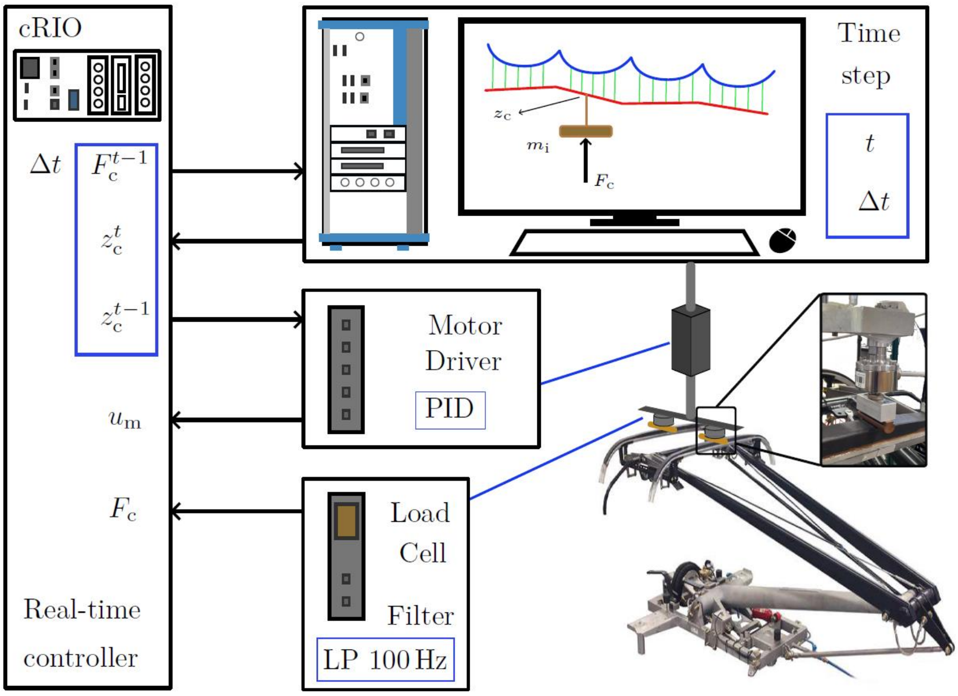

Figure 1: Scheme of the Hardware-in-the-Loop components and workflow.

1. DSA-380 pantograph
2. Vertical linear motor
3. Motor and guides for lateral displacement
4. Load cells
5. Real-time Speedgoat PC
6. Accelerometers
7. Pneumatic circuit
8. High-speed camera

Figure 2: Hardware-in-the-Loop test rig.

2.2 Catenary model

Figure 1 depicts a section of a catenary finite element model. Dots in the contact wire schematically represent three potential interaction points with the pantograph at given time steps, $t=1,\ldots,N_t$. The vehicle speed V is constant so it is the distance between points. Vector $\mathbf{f}_c$ contains the external applied force in the contact wire in all time steps, so that component t of this vector $\mathbf{f}_{c\_t}$, is the force applied on point t and time step t. Assuming a linear behaviour of the catenary, the dynamic response can be obtained using convolution from the applied contact force. The height of point t of the contact wire at time step t is stored in the t-th component of vector $\mathbf{z}_c$ ($\mathbf{z}_{c\_t}$). This vector can be obtained from the force using the impulse response matrix $\mathbf{I}_{cc}$ and the initial position of the contact wire $\mathbf{z}_0$ as:

$$\mathbf{z}_c = \mathbf{z}_0 + \mathbf{I}_{cc} \cdot \mathbf{f}_c \tag{1}$$

The impulse response matrix has been obtained using the catenary model presented in [6], for a unit impulse force, for the time step of Dt = 2ms, and assuming that droppers behave linearly.

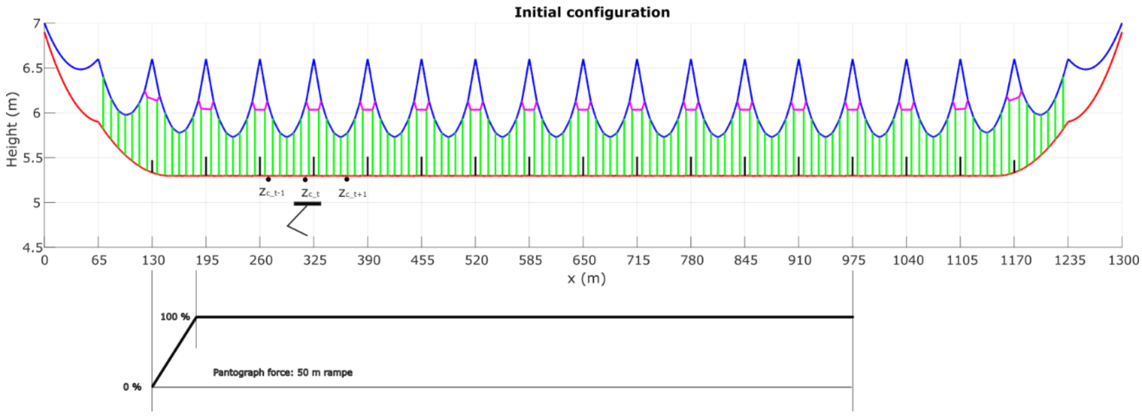

Figure 3: Stitch-wire catenary section with 20 spans. Pantograph force is gradually introduced from span 3.

2.3 Model Predictive Control Design

In addition to the catenary, the motor, the pantograph and their interaction have to be modelled for the Model Predictive Controller design. The linear motor driver receives the reference position of the catenary each time step. Assuming a linear model, the position of the motor slider each time step $\mathbf{z}_{m\_t}$ depends on the catenary position. Using convolution and the impulse response matrix of the motor $\mathbf{I}_{mc}$, the position vector of the motor can be obtained as:

$$\mathbf{z}_m = \mathbf{I}_{mc} \cdot \mathbf{z}_c \tag{2}$$

The motor interacts with a real pantograph through contact pads with stiffness k_h. Using a linear lumped mass model of the pantograph the position of the upper mass of the model with respect to the initial equilibrium position in all time steps $\mathbf{z}_u$ depends on the motor position, and can be obtained with the impulse response of the pantograph $\mathbf{I}_{um}$ as:

$$\mathbf{z}_{\mathrm{u}} = \mathbf{I}_{\mathrm{um}} \cdot \mathbf{z}_{\mathrm{m}} \tag{3}$$

The contact force is computed from the contact stiffness as:

$$\mathbf{f}_{\mathrm{c}} = k_h\left(\mathbf{z}_{\mathrm{m}} - \mathbf{z}_{\mathrm{u}}\right) = k_h\left(\mathbf{I} - \mathbf{I}_{\mathrm{um}}\right)\mathbf{z}_{\mathrm{m}} = \mathbf{I}_{\mathrm{pm}} \cdot \mathbf{z}_{\mathrm{m}} \tag{4}$$

To find the MPC controller, the full system is expressed in state space form. The controller action $\mathbf{u}_{\mathrm{mpc}}$ is sent to the motor, modifying Eq (2). Superscript *t* on vectors $\mathbf{f}_{\mathrm{c}}$, $\mathbf{z}_{\mathrm{c}}$ and $\mathbf{z}_{\mathrm{m}}$ denotes that the components of the vector from first to *t*-th remain the same in subsequent iterations. The state space equations are written for components $k=1,\ldots,N_t$ as:

$$\begin{aligned}
\mathbf{z}^{\mathrm{t}}_{\mathrm{c_k}} &= \mathbf{z}^{\mathrm{t-1}}_{\mathrm{c_k}} + \mathbf{I}_{\mathrm{cc_k,t-1}} \cdot \mathbf{f}^{\mathrm{t-1}}_{\mathrm{c_t-1}} \\
\mathbf{z}^{\mathrm{t}}_{\mathrm{m_k}} &= \mathbf{z}^{\mathrm{t-1}}_{\mathrm{m_k}} + \mathbf{I}_{\mathrm{mc_k,t-1}} \cdot \mathbf{z}^{\mathrm{t-1}}_{\mathrm{c_t-1}} + \mathbf{I}_{\mathrm{mc_k,t}} \cdot \mathbf{u}_{\mathrm{mpc,t}} \\
\mathbf{f}^{\mathrm{t}}_{\mathrm{c_k}} &= \mathbf{f}^{\mathrm{t-1}}_{\mathrm{c_k}} + \mathbf{I}_{\mathrm{pm_k,t-1}} \cdot \mathbf{z}^{\mathrm{t}}_{\mathrm{m_t}}
\end{aligned} \tag{5}$$

Eq. (5) can be rearranged in matrix form as:

$$\mathbf{x}^{\mathrm{t}} = \mathbf{A}^{\mathrm{t-1}} \cdot \mathbf{x}^{\mathrm{t-1}} + \mathbf{b}^{\mathrm{t-1}} \cdot \mathbf{u}_{\mathrm{mpc,t}} \qquad \text{where} \quad \mathbf{x}^{\mathrm{t}} = \begin{Bmatrix} \mathbf{z}^{\mathrm{t}}_{\mathrm{c}} \\ \mathbf{z}^{\mathrm{t}}_{\mathrm{m}} \\ \mathbf{f}^{\mathrm{t}}_{\mathrm{c}} \end{Bmatrix} \tag{6}$$

Eq. (6) is used to predict the system response the next *N* steps, from the state $\mathbf{x}^{\mathrm{t-1}}$, and the controller action is computed to optimize the following quadratic cost function:

$$J = \sum_{i=1}^{N} \mathbf{x}^{\mathrm{t+i\,T}} \cdot \mathbf{Q}^{\mathrm{t+i}} \cdot \mathbf{x}^{\mathrm{t+i}} + \sum_{i=1}^{N} \mathbf{u}^{\mathrm{T}}_{\mathrm{mpc}} \cdot \mathbf{R}^{\mathrm{t+i}} \cdot \mathbf{u}_{\mathrm{mpc}} \tag{7}$$

The weighting matrix **Q** penalizes the difference between the catenary position reference and the real motor position, $\mathbf{z}_{\mathrm{c}}$-$\mathbf{z}_{\mathrm{m}}$ each time step. Matrix **R** penalizes the control action. Both the position error and the action can be filtered by properly defining these matrices.

The solution of the optimization problem of Equation (7) subject to Equation (6), determines the optimal controller action $\mathbf{u}_{\mathrm{mpc}}$. Only the first component is sent to the motor and the optimisation problem is solved again after updating the state vector of the system. As the system model is linear, the optimal controller is a linear function of the state:

$$\mathbf{u}_{\mathrm{mpc,t}} = \mathbf{K}^{\mathrm{t}}_{\mathrm{mpc}}\, \mathbf{x}^{\mathrm{t}} \tag{8}$$

Matrix $\mathbf{K}_{\mathrm{mpc}}$ can be precomputed in an offline stage and used in the real time controller during test.

3 Results

The catenary model used to test the proposed methods is shown in Figure 3. The complete catenary section has 20 spans of L = 65m span length. The first and last two spans are transition spans, while every internal span has 7 droppers and a stitch wire. The pantograph interaction is gradually introduced from span number 3, with a 50 m ramp in which the pantograph force is linearly increased. A constant speed of the vehicle V=300 km/h is considered in the tests.

DSA-380 pantograph model is tested with the virtual catenary for T=10 s, i.e. 5000 time steps using the proposed methodology with the MPC controller. The contact force and the position of the contact point are recorded.

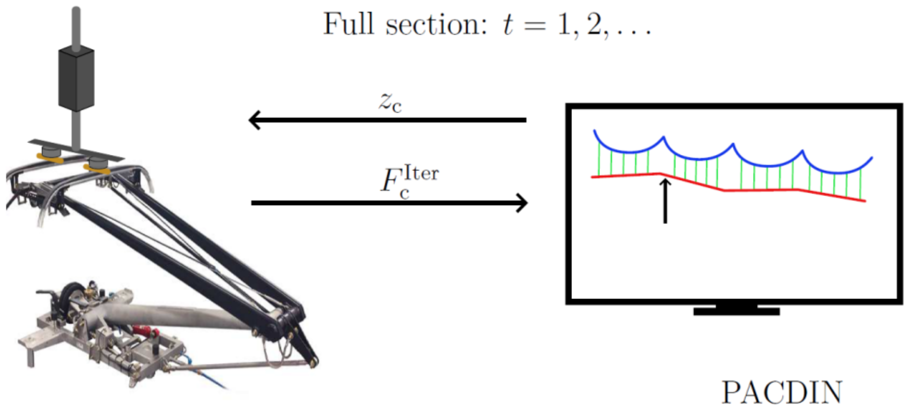

Figure 4: Iterative HiL test.

A reference solution of the interaction between the real pantograph and the catenary is used to validate the proposed method. To obtain this reference solution, we follow the iterative procedure explained in [5] and schematically shown in Figure 4. The contact force F_c^1 is applied to the catenary model as an external force to compute offline the contact position, z_c^1. This position is sent to the linear motor and a new contact force is obtained F_c^2. The iterative process is performed until convergence, i.e. the contact position does not change in two consecutive iterations.

The contact force from the HiL test, and the reference solutions are compared in Figure 5, both in time and frequency domains. The position of the contact point is compared in Figure 6. The maximum difference in the position is about 1 mm.

The response of the catenary given an external action F_c depends on the impulse response I_{cc} and the static configuration of the contact wire z_0, as shown in Equation (1). This real-time model neglects the dropper slackening. The contact wire height profile used in the previous test is the nominal configuration of the catenary, with the exact height in the dropper connections. During the catenary installation, technicians can make small mistakes that lead to a different static configuration from the original design. In reference [8] the influence of uncertainties introduced during catenary installation was analysed and a method to obtain z_0 was proposed. Using this method, several contact wire profiles have been generated, and used for HiL testing with the real pantograph. The contact force results from 10 HiL tests are compared with that of the nominal configuration in Figure 8. The standard deviation of the filtered contact force in the 5 central spans ranges from 27.0 N to 29.0 N. The value for the nominal configuration is 26.8 N. Figure 8 shows similar frequency content for all tests, with the dropper passing frequency being the most relevant.

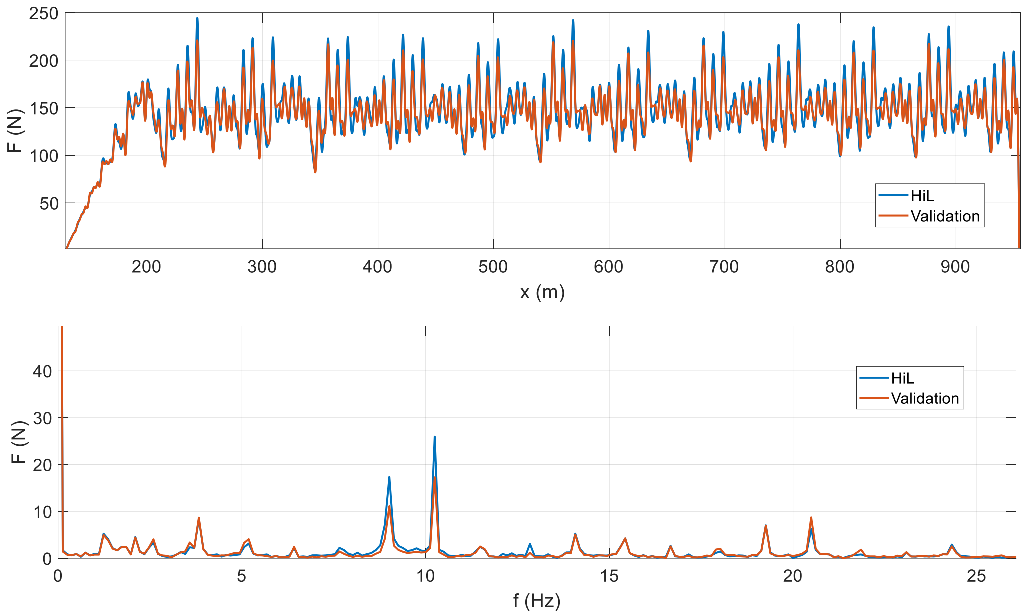

Figure 5: Comparison of the contact force in the HiL test in time and frequency.

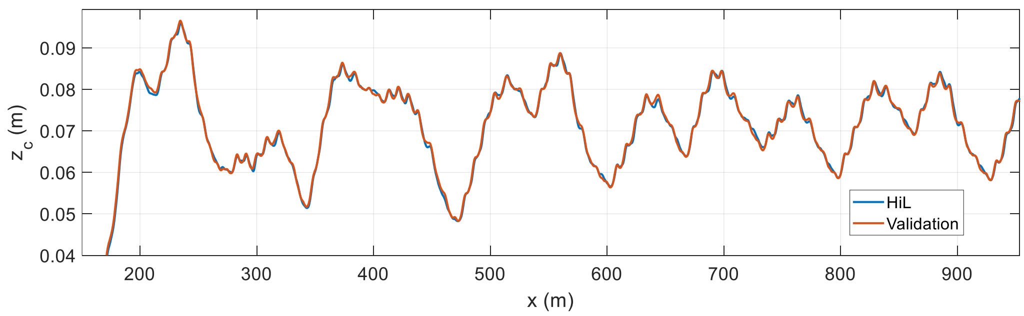

Figure 6: Comparison of the contact point position in the HiL test.

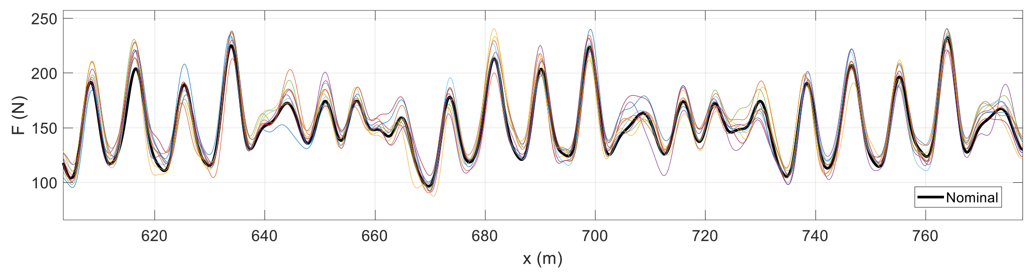

Figure 7: Contact force in the HiL test for different contact wire profiles. The black line shows the nominal configuration results.

4 Conclusions and Contributions

In this work, a new method is proposed to perform HiL tests of pantographs. The catenary model is linear based on the impulse response to external forces. In the experimental setup, delays occur due to communication between the motor drive, acquisition system, and simulation PC. An MPC controller is proposed to compensate for delays and stabilise the system. For the catenary model used, the controller is a linear function of the state that can be precomputed in an offline stage. Laboratory tests show that the proposed controller stabilises the system.

The contact force obtained in the HiL test has been compared with a reference solution showing acceptable results in the 0 to 20 Hz frequency range. The difference achieved by the motor with respect to the contact wire reference is smaller than 1mm.

Contact wire profiles have been generated considering possible catenary installation errors, and HiL tests have been carried out to compare the contact force. In general, the standard deviation of the contact force is up to 10% higher than that of the nominal catenary.

Future work will improve the catenary model adding a correction force to consider non-linear dropper behavior due to slackening.

Acknowledgements

The authors wish to express their gratitude for the financial support received from Grant PID2020-113458RBI00 funded by MCIN/AEI/10.13039/501100011033 and Valencian Regional Government (PROMETEO/2021/046).

References

[1] A. Facchinetti, S. Bruni, Hardware-in-the-loop hybrid simulation of pantograph–catenary interaction, Journal of Sound and Vibration 331 (1–12) 2783–2797, 2012.

[2] A. Schirrer, G. Aschauer, E. Talic, M. Kozek, S. Jakubek, Catenary emulation for hardware-in-the-loop pantograph testing with a model predictive energy-conserving control algorithm, Mechatronics 41, 17 – 28, 2017.

[3] S. Kobayashi, D. P. Stoten, Y. Yamashita, T. Usuda, Dynamically substructured testing of railway pantograph/catenary system, Proceedings of the Institution of Mechanical Engineers, Part F: Journal of Rail and Rapid Transit. 233 (5). 516–525, 2019.

[4] J. Gil, M. Tur, S. Gregori, A. Correcher, A.M. Pedrosa, F.J. Fuenmayor, Hardware-in-the-Loop simulations of a railway pantograph with a finite element periodic catenary model, Vehicle System Dynamics, 1–24, 2023.

[5] M. Tur, S. Gregori, C. Antonio, J. Gil, P. Ana, J. Fuenmayor. An LQG controller for HiL pantograph test. Zenodo. https://doi.org/10.5281/zenodo.10582338, 2024.

[6] S. Gregori, M. Tur, E. Nadal, J. Aguado, F. J. Fuenmayor, P. Chinesta, Fast simulation of the pantograph–catenary dynamic interaction, Finite Elements in Analysis and Design 129, 1-13, 2017.

[7] A. Schirrer, J. Santos, M. Grujic, J. Zulehner, M. Weichselbaumer, P. Antunes, J. Pombo, C. Hametner, S. Jakubek, Time delay in a mechatronic Power-HIL system: Analysis and model-based compensation, Control Engineering Practice, 144 (2024) 105832

[8] S. Gregori, M. Tur, J.E. Tarancón, F. J. Fuenmayor, Stochastic Monte Carlo simulations of the pantograph–catenary dynamic interaction to allow for uncertainties introduced during catenary installation, Vehicle System Dynamics 57, 471-492, 2019.